Inductive Sensing Technique For Low Power Implantable Hydrogel-Based Biochemcial Sensors

Yuechuan Yu, Vishal Bhola, Prashant Tathireddy, Darrin J. Young
Department of Electrical and Computer Engineering
University of Utah
Salt Lake City, Utah, USA

Shad Roundy
Department of Mechanical Engineering
University of Utah
Salt Lake City, Utah, USA

Abstract—**This paper presents the feasibility study and investigation of an inductive sensing technique with respect to the swelling of hydrogel samples for implantable biochemical sensing applications. A prototype sensing system is implemented based on an ultra-low power tunnel diode oscillator employing a 3 mm-diameter, 10-turn sensing coil positioned at 100 µm away from a 5 mm x 5 mm metallic sensing plate adhered to a hydrogel slab surface. The oscillator achieves a nominal frequency of approximately 28 MHz with a sensitivity of 15 KHz per um of hydrogel displacement while dissipating a DC power of 40 µW. Further characterization with hydrogel samples immersed in DI water demonstrates that the sensing system can detect 29 µm swelling of the hydrogel along vertical direction.**

Keywords—Inductive Sensing, Wireless Sensing, Tunnel Diode Oscillator, Hydrogel, Hydrogel-Based Glucose Sensor, Low Power Implant, Biomedical Implant.

I. INTRODUCTION

It is highly desirable to develop deeply implantable hydrogel-based wireless sensing capability to capture *in vivo* biochemical parameters such as glucose, pH, and ionic strength [1-4]. Advancement in MEMS technology has enabled the realization of cubic mm size complex systems [5-7]. However, energy sources, power dissipation, and reliable packaging impose severe challenges for realizing miniature long-term implantable sensors. This paper presents a proposed novel deeply implantable wireless intraluminal glucose sensing architecture depicted in Figure 1, where the implantable sensor exhibiting a dimension of approximately 5 mm x 3 mm x 1 mm is implanted inside a blood vessel. The sensor can be powered by an ultrasonic power source across the skin and tissue [8-10]. Glucose concentration inside the vessel can be sensed by an inductive sensing technique employing a glucose-sensitive hydrogel embedding a miniature metallic sensing plate. Functionalized glucose-sensitive hydrogels can reversibly change in volume proportional to the change in glucose concentration [1, 2, 11], which causes a displacement of the embedded metallic sensing plate that can be detected by the inductance change of a sensing coil placed in a close proximity. This sensing method can potentially overcome several key limitations plaguing traditional enzymatic continuous glucose sensors and high-impedance capacitance-based glucose sensors that are prone to leakage [12-13]. Furthermore, the proposed sensing technique allows the sensing coil and associated electronics to be robustly encapsulated in a hermetically-sealed glass package due to the sensing configuration that a direct contact between the coil and hydrogel is not required, attractive for long-term implant applications.

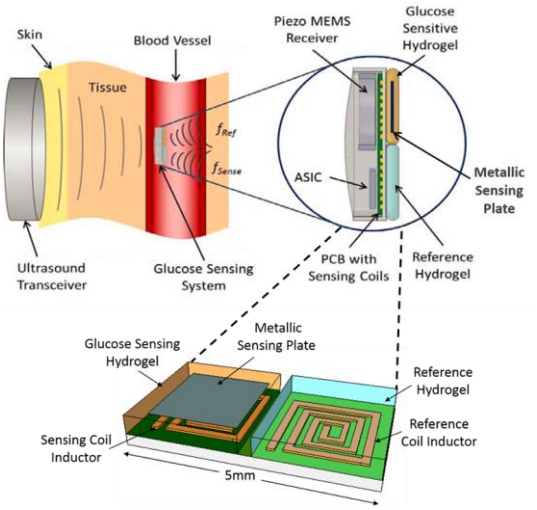

Fig. 1. Wireless implantable hydrogel-based glucose sensing architecture.

The sensing coil employed as a part of an LC tank circuit can effectively modulate the frequency of an RF oscillator, thus wirelessly transmitting the sensor information to an external receiver. A tunnel diode oscillator architecture is chosen due to its ultra-low power dissipation [14], critical for implant applications where power sources are highly constrained. As depicted in Figure 1, a non-glucose-sensitive reference hydrogel (without showing an embedded metallic sensing plate on top for simplicity of illustration) and a reference coil inductor are adjacently incorporated in the design, serving as a reference frequency for calibration purpose. This technique is highly desirable for eliminating base-line drift caused by environmental effects. A single tunnel diode (TD) will be employed for generating f_{Sense} and f_{Ref} to ensure a consistent diode characteristic used in the both oscillators as illustrated in the overall electrical system design shown in Figure 2, where a front-end MEMS PZT power generator converts the incoming acoustic power to a DC

978-1-4799-8203-5/15/$31.00 ©2015 IEEE

supply voltage, which energizes the tunnel-diode oscillators and logic control circuits. This paper focuses on the feasibility study and investigation of the proposed inductive sensing technique with respect to the swelling of hydrogel samples in solution and ultra-low power wireless telemetry system design.

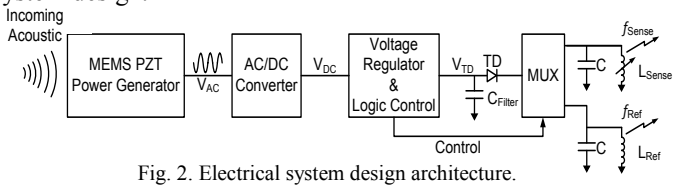

Fig. 2. Electrical system design architecture.

II. INDCUTIVE SENSING AND CHARACTERIZATION

A prototype 3 mm-diameter, 10-turn coil inductor exhibiting an inductance value of approximately 500 nH was constructed to conduct the inductive sensing characterization and feasibility study. Further miniaturized 1 mm-diameter inductor will be designed and fabricated in an ASIC form for the final system implementation. Figure 3 presents a photo of the inductive sensing characterization setup, where a 5 mm x 5 mm metallic sensing plate is positioned above the sensing coil with an adjustable gap size controlled by a micro-manipulator.

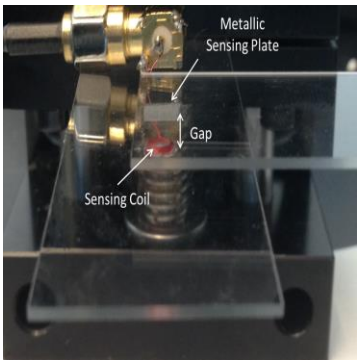

Fig. 3. Inductive sensing characterization setup.

The sensing coil exhibits an inductance of approximately 386 nH with an initial gap size of 100 µm from the sensing plate. An increased gap size from the initial offset results in an increased inductance due to reduced Eddy current effects as plotted in Figure 4, revealing a sensitivity of 4 nH/10 µm.

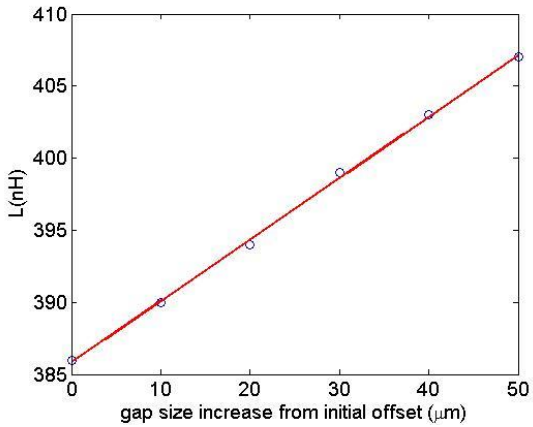

Fig. 4. Inductance vs. gap size from initial offset.

The sensing coil was then coated with a 10 µm-thick parylene film as a biocompatible insulating layer, followed by the inductive sensing characterization performed in saline solution and DI water. The experimental results revealed a similar performance as shown in Figure 4.

The RF characteristics of the sensing coil were also evaluated. Figure 5 presents the measured coil inductance value versus frequency in air and in saline solution with a parallel metallic sensing plate positioned 100 µm apart. The sensing coil exhibits a self-resonance above 70 MHz in saline.

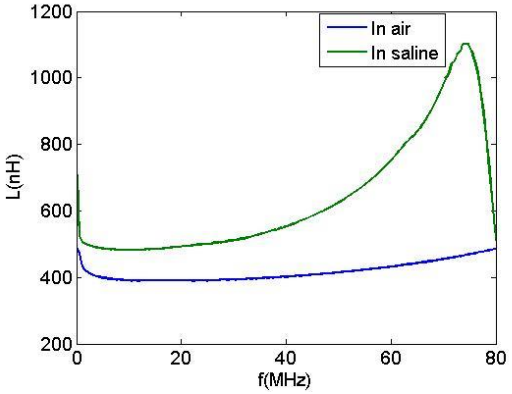

Fig. 5. Measured coil inductance vs. frequency.

Figure 6 presents the measured sensing coil quality factor (Q) versus frequency, revealing the maximum Q of 20 and 45 at 40 MHz and 60 MHz in saline solution and in air, respectively. The quality factor is a critical parameter associated with the loss of the coil inductor for the oscillator design described in the following section.

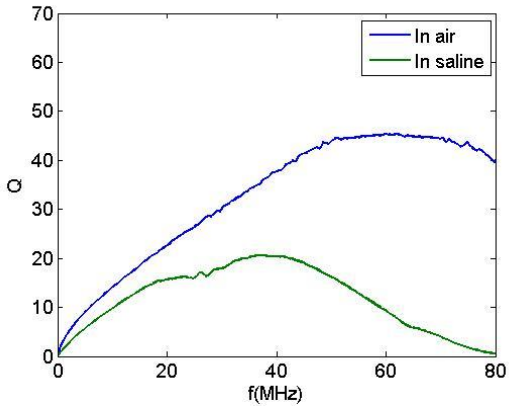

Fig. 6. Sensing coil Q value vs. frequency in saline and in air.

III. LOW POWER TUNNEL DIODE OSCILLATOR DESIGN AND CHACTERIZTAION

Figure 7 presents a general tunnel diode oscillator design topology, where a low DC bias voltage around 200 mV is used to bias the tunnel diode to achieve an adequate negative resistance required for the oscillator design. The resonant frequency of the LC tank circuit sets the steady-state oscillation frequency. The change of the sensing coil inductance value, therefore, modulates the steady-state oscillation frequency. The sensing coil also acts as a transmission antenna to wirelessly

transmit the oscillation signal, i.e. the sensor information, to a nearby receiver.

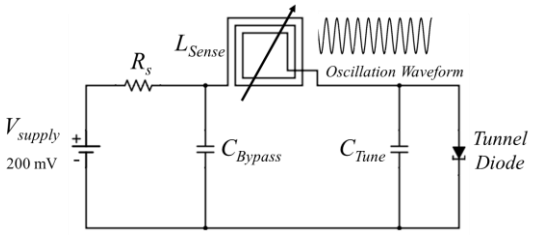

Fig. 7. Tunnel diode oscillator design topology.

A commercial silicon tunnel diode is employed for the prototype oscillator design. Figure 8 presents the measured I-V characteristics of the tunnel diode, achieving a negative resistance of around –1500 Ω at the bias voltage of 200 mV. The negative resistance is sufficient to compensate the loss of the LC tank circuit mainly dominated by the loss of the sensing coil, thus ensuring a reliable oscillation start up. It should be noted that the tunnel diode dissipates a DC current of approximately 200 µA at the bias voltage of 200 mV, corresponding to an ultra-low power consumption of only 40 µW, which is critical for a deep implant with a highly constrained power source.

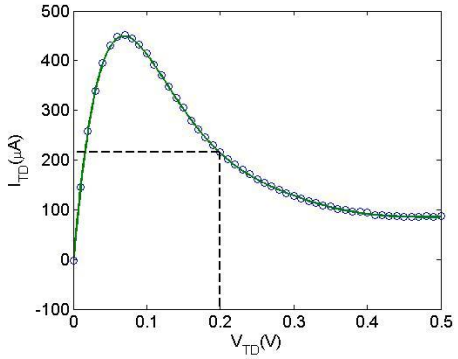

Fig. 8. I-V characteristics of tunnel diode.

A prototype tunnel diode oscillator was implemented to achieve a nominal frequency of 28.4 MHz, close to the designed frequency where the maximum Q occurs in saline solution. Figure 9 presents the wirelessly measured oscillator output power spectrum with an RF power of -67 dBm.

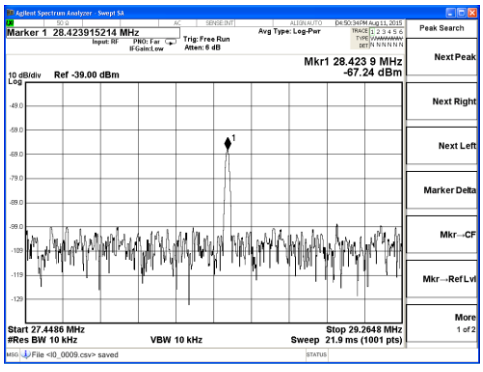

Fig. 9. Measured oscillator output power spectrum.

The oscillator output frequency can be varied from 27.81 MHz to 28.58 MHz over a 50 µm gap size change between the sensing coil and metallic sensing plate in saline solution as shown in Figure 10.

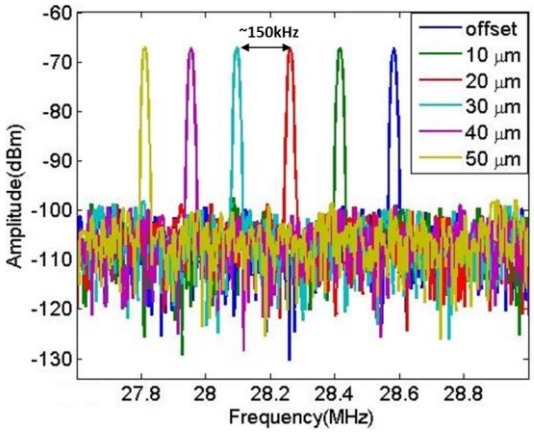

Fig. 10. Oscillator output frequency shift over 50 µm gap size change.

The demonstrated sensitivity of approximately 15 KHz per µm displacement closely matches the inductance sensitivity reported in Figure 4. The oscillator frequency stability was characterized over a period of 72 hours, exhibiting a peak-to-peak variation of 3 KHz, corresponding a displacement sensing resolution of 0.2 µm. Wireless telemetry performance was also evaluated by employing a 10 mm-diameter receiver coil attached to the input of a spectrum analyzer. Figure 11 shows the received RF power spectrum at 10 cm telemetry distance, indicating an RF power of -118 dBm at 32.2 MHz with a signal-to-noise ratio (SNR) of approximately 10 dB. The demonstrated telemetry distance is sufficient for the proposed deep implant application.

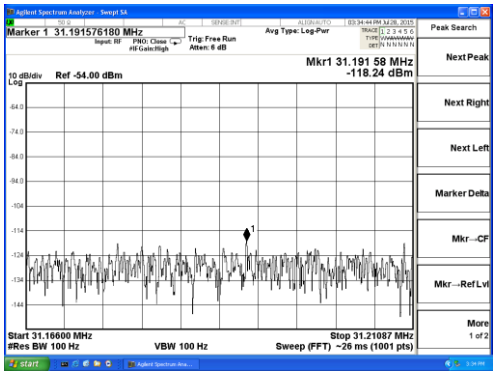

Fig. 11. Wirelessly received power spectrum at 10 cm telemetry distance.

IV. INDUCTIVE SENSING FOR HYDROGEL-BASED SENSOR

The proposed inductive sensing method was characterized with a hydrogel sample containing a metallic sensing plate on top in DI water to demonstrate the detection of inductance change and the resulting oscillator frequency variation as the hydrogel volume swells. Figure 12 shows a photo of the experimental setup. A 5 mm x 5 mm metallic sensing plate with a thickness of 10 µm was first adhered to the surface of a hydrogel slab, exhibiting a dimension of 8 mm x 8mm x 400 µm, by using a gel-bond film. The hydrogel slab was then

immersed in 1XPBS solution to reach an equilibrium, followed by transferring the sample to a different testing container.

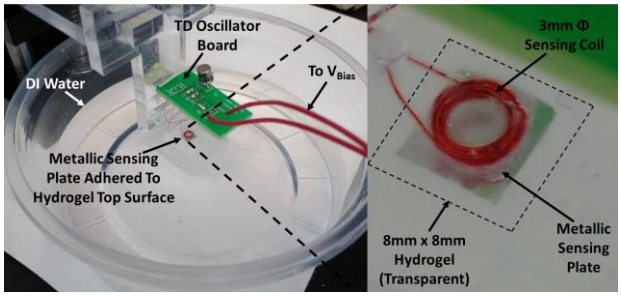

Fig. 12. Test setup for inductive sensing with hydrogel.

A 3 mm-diameter sensing coil was then positioned above the hydrogel slab surface with a 100 µm air gap controlled by a micro-manipulator. The coil is connected to the tunnel diode oscillator electronics implemented on a PCB as shown in the figure. At this point, DI water was added into the container to immerse the hydrogel slab as well as the sensing coil. The increased water content in the hydrogel causes a swelling of the slab, thus reducing the gap size between the metallic sensing plate and sensing coil, which results in a decreased coil inductance value and an increased oscillation frequency. Figure 13 presents the wirelessly measured oscillator power spectrum over a 15-minute time period starting from the DI water filling into the testing container. The frequency is shifted from 28.37 MHz to 28.8 MHz over the 15-min time duration. Correlating with the plot shown in Figure 4 indicates the swelling of hydrogel slab by approximately 29 µm along the vertical direction.

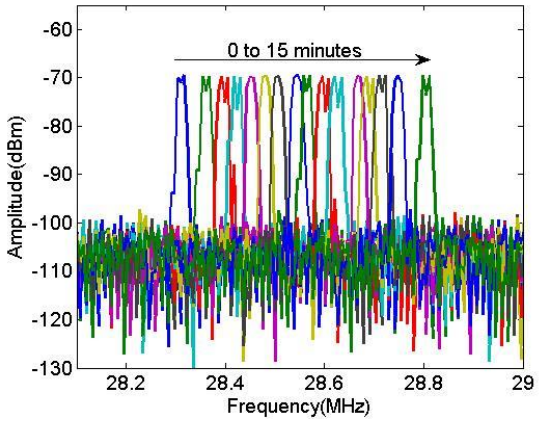

Fig 13. Oscillator output frequency shift due to swelling of hydrogel.

The demonstrated sensing performance confirms the feasibility of the proposed inductive sensing technique coupled with a hydrogel whose volume is sensitive to external stimuli. Functionalized glucose-responsive hydrogels are currently under preparation for testing in a controlled glucose concentration environment, planned as the next step.

V. CONCLUSIONS

The proposed inductive sensing technique with respect to the swelling of hydrogel samples in solution has been demonstrated. A prototype sensing system employing an ultra-low power tunnel diode oscillator achieves a nominal frequency of approximately 28 MHz with a sensitivity of 15 KHz per um of hydrogel displacement while dissipating a DC power of 40 µW. Frequency stability test indicates an achievable displacement sensing resolution of 0.2 µm. The demonstrated sensing performance is expected to enable the realization of a deeply implantable hydrogel-based wireless intraluminal glucose sensor.

ACKNOWLEDGMENT

This research is supported by the National Science Foundation under grant number: ECCS-1408265.

P. Tathireddy has commercial interest in Applied Biosensors, LLC.

REFERENCES

[1] M. Lei, A. Baldi, E. Nuxoll, R.A. Siegel, B. Ziaie, "Hydrogel-based microsensors for wireless chemcial monitoring," *Biomedical Microdevice*, 2009, 11:529-538.

[2] Christie M. Hassan, Francis J. Doyle III, and Nikolaos A. Peppas, "Dynamic Behavior of Glucose-Responsive Poly(methacrylicacid-g-ethylene glycol) Hydrogels," *Macromolecules,* 1997, 30, 6166 - 6173.

[3] Jeong-Il Kim, Zhenwen Ding, Sang-No Lee, Jong-Gwan Yook, and Dimitrios Peroulis, "Hydrogel-Based Integrated Antenna-pH Sensor," *Proc. IEEE Sensors Conf.*, Oct., 2007, pp 695 – 698.

[4] M. Avula, N. Busche, S.H. Cho, P. Tathireddy, L.W. Rieth, J.J. Magda, F. Solzbacher, "Effect of Temperature Changes on the Performance of Ionic Strength Biosensors Based on Hydrogels and Pressure Sensors," *Proc. IEEE Eng. Med. Biol. Soc*., Sep. 2011, pp. 10–13.

[5] A. Branner and R.A. Normann, "A multielectrode array for intrafascicular recording and stimulation in sciatic nerve of cats," *Brain Res Bull*, 2000. 51(4): pp. 293-306.

[6] P. Cong, N. Chaimanonart, W. H. Ko, and D. J. Young, "A Wireless and Batteryless 10-bit Implantable Blood Pressure Sensing Microsystem with Adaptive RF Powering for Real-time Genetically Engineered Mice Monitoring," *IEEE Journal of Solid-State Circuits,* Vol. 44, No. 12, pp. 3631-3644 (Special Issue), December 2009.

[7] S. A. Zotov, M. C. Rivers, A. A. Trusov, A. M. Shkel, "Folded-MEMS-Pyramid Inertial Measurement Unit," *IEEE Sensors Journal*, *Vol*.11, *No*.11, pp.2780-2789, November 2011.

[8] D. Seo, J. M. Carmena, J. M. Rabaey, M. M. Maharbiz, E. Alon, "Model validation of untethered, ultrasonic nerual dust motes for cortical recording," *Journal of Neuroscience Mothods*, 244 (2015), 114-122.

[9] D. Seo, J. M. Carmena, J. M. Rabaey, E. Alon, M. M. Maharbiz, " Nural Dust: An Ultrasonic, Low Power Solution for Chronics Brain-Machine Interfaces," ArXiv e-prints, July 2013.

[10] J. Zhou, A. Kim, S. H. Song and B. Ziaie, "An Ultrasonically Powered Implantable Micro-Light Source For Localized Photodynamic Therapy," *the 18th International Conference on Solid-State Sensors, Actuators and Microsystems*, Anchorage, Alaska, U.S.A., June, 2015, pp. 876-879.

[11] M. Lei, B. Ziaie, E. Nuxoll, K. Iván, Z. Noszticzius, and R.A. Siegel, "Integration of Hydrogels with Hard and Soft Microstructures," *Journal of Nanoscience and Nanotechnology*. Vol. 7, 2007, pp780-789.

[12] N. S. Oliver, C. Toumazou, A. E. G. Cass and D. G. Johnston, "Glucose sensors: a review of current and emerging technology," *Diabetic Medicine*, December, pp. 1464-5491, 2008.

[13] P-H Kuo, S-S Lu, J-C Kuo, Y-J Yang, T. Wang, Y-L Ho and M-F Chen, "A Hydrogel-Based Implantable Wireless CMOS Glucose Sensor SoC," *IEEE International Symposium on Circuits and Systems*, Seoul, Korea, 2012, pp. 994-997.

[14] M. Suster, W. H. Ko, D. J. Young, "An Optically-Powered Wireless Telemetry Module for High-Temperature MEMS Sensing and Communication," *IEEE Journal of Microelectromechanical Systems,* June, pp. 536-541, 2004.